

Local and noncontact measurements of bulk acoustic wave velocities in thin isotropic plates and shells using zero group velocity Lamb modes

Dominique Clorennec, Claire Prada,^{a)} and Daniel Royer

Laboratoire Ondes et Acoustique, ESPCI, Université Paris 7, CNRS UMR 7587, 10 rue Vauquelin, 75231 Paris Cedex 05, France

(Received 8 September 2006; accepted 3 December 2006; published online 8 February 2007)

An original method for material characterization with acoustic waves is presented. The measurement of the longitudinal and shear wave velocities in thin isotropic plates or shells is performed locally on the same face without any mechanical contact. We exploit the resonance that occurs at the minimum frequency thickness product of the first order symmetric (S_1) and of the second order antisymmetric (A_2) Lamb modes. At these frequencies the group velocity vanishes, whereas the phase velocity remains finite. Then, the energy, which cannot propagate in the structure, is localized in a zone of diameter half the wavelength. The vibrations are excited in the thermoelastic regime by a laser pulse and detected at the same point by an optical interferometer. For these two Lamb modes we have computed the variations of the frequency thickness product versus Poisson's ratio. The resonance frequency ratio, which is independent of the plate or shell thickness, provides an absolute and local measurement of Poisson's ratio. Provided that the plate thickness is known, each resonance frequency allows us to determine in a single shot the bulk acoustic wave velocities V_L and V_T . Since it is based on frequency measurements, the method, tested on a large number of materials, is very accurate. © 2007 American Institute of Physics.

[DOI: [10.1063/1.2434824](https://doi.org/10.1063/1.2434824)]

I. INTRODUCTION

Characterization of mechanical properties of materials is important for testing their structural integrity. Nondestructive evaluation of these properties is usually carried out with ultrasonic waves. When there is only access to one face of the sample, pulse-echo techniques are widely used for determining bulk acoustic wave (BAW) velocities. Depending on the structure to evaluate and on the frequency domain, different techniques have been developed. For concrete applications and in the kilohertz range, a mechanical impactor is used. This impact-echo (IE) method, based on the concept of multiple reflections of longitudinal waves between the top and bottom faces of the structural element under test, has been developed over the past 20 years.¹ For metallic or composite structures, the ultrasonic emitter and receiver is a single longitudinal or transverse piezoelectric transducer working in the megahertz range.^{2,3} Surface acoustic waves (SAWs) have also been extensively exploited for near-surface evaluation of materials. For a local investigation, scanning acoustic microscopes have been developed in the 10 MHz to 1 GHz frequency range.⁴ All these techniques need a mechanical contact with the structure or the material under test.

In the case of a plate or of a thin hollow cylinder, another approach is to exploit Lamb waves, i.e., elastic waves guided by the structure. The propagation of these symmetric (S) and antisymmetric (A) modes is represented by a set of dispersion curves giving the angular frequency ω versus the wave number k .^{5,6} Noncontact ultrasonic methods using the

generation and detection of zero-order symmetric (S_0) and antisymmetric (A_0) Lamb modes by lasers in thin metal sheets⁷ or in hollow cylinders⁸ have been investigated. The characterization method, based on the observation of the spreading of the wave train due to the dispersion of the A_0 Lamb mode, needs a rather large propagation distance. The measurement is not local and experiments show that the uncertainty (2%–20%) increases with the wall thickness d (typically 0.05–1 mm). Using a space-time Fourier transform and a fit of the A_0 and S_0 dispersion curves, Gao *et al.* determine the thickness and the bulk acoustic wave velocities of a thin copper sheet with a better accuracy.⁹ Another way of measuring dispersion curves consists in using phase-mask technology.¹⁰ However, those methods need measurement on a large area of the sample and so are nonlocal techniques.

Some higher order Lamb modes exhibit an anomalous behavior at frequencies where the group velocity $V_g = d\omega/dk$ vanishes while the phase velocity $V_\phi = \omega/k$ remains finite. At this zero group velocity (ZGV) point the energy, which cannot propagate in the plate, is trapped under the source. This sharp and local resonance effect was first observed with the first order symmetric (S_1) Lamb mode. For example, using focusing, air-coupled transducers, Holland and Chimenti¹¹ found an efficient transmission of airborne sound waves through a thick plate at the S_1 -ZGV resonance frequency. Gibson and Popovics demonstrated that the resonance excited in concrete by mechanical impacts (IE method) corresponds to the S_1 -ZGV frequency.¹² Similar result was obtained, independently, by Prada *et al.* in the case of a thin tungsten sheet mechanically excited at 45 MHz by

^{a)}Electronic mail: claire.prada-julia@espci.fr

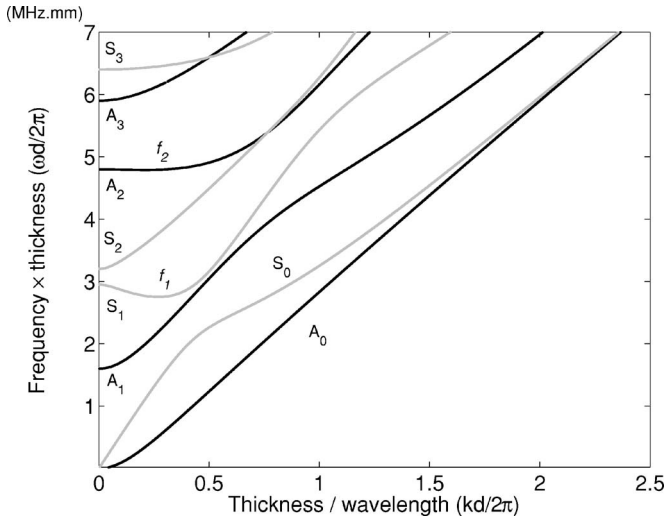


FIG. 1. Lamb wave dispersion curves for a steel plate of thickness d and bulk wave velocities equal to $V_L=5900$ m/s and $V_T=3200$ m/s. Vertical scale: $fd=\omega d/2\pi$; horizontal scale: $d/\lambda=kd/2\pi$.

an intensity modulated laser diode and detected with an optical interferometer at the same point of the plate.¹³ Recently, it has been shown that the S_1 -ZGV resonance can also be excited by a laser pulse and optically detected in the time domain.¹⁴

Mechanical vibrations involved with the first order symmetric Lamb mode at the ZGV point are mainly of longitudinal type. With a laser source, the same phenomenon involving transverse vibrations can be observed for the second antisymmetric (A_2) Lamb mode. In this paper it will be demonstrated that the simultaneous measurement of these two (ZGV)-resonance frequencies provides an accurate and local determination of Poisson's ratio ν and, if the plate thickness d is known, of the longitudinal and transverse acoustic wave velocities V_L and V_T .

II. ANALYSIS

Elastic properties of an isotropic material are characterized by two constants c_{11} and c_{12} . However, Lamb wave propagation can be expressed in terms of only one dimensionless parameter, the bulk wave velocity ratio $\kappa=V_L/V_T$ or Poisson's ratio ν :

$$\kappa = \frac{V_L}{V_T} = \sqrt{\frac{2(1-\nu)}{1-2\nu}}. \quad (1)$$

As an example, Fig. 1 shows the dispersion curves for the first four symmetric and antisymmetric modes propagating in a steel-free plate of thickness d . The longitudinal and transverse bulk wave velocities are equal to $V_L=5900$ m/s and $V_T=3200$ m/s, respectively ($\nu=0.2916$), and we have plotted the variations of the frequency thickness product ($fd=\omega d/2\pi$) versus the thickness to wavelength ratio ($d/\lambda=kd/2\pi$).

The fundamental modes A_0 and S_0 do not exhibit any cutoff when the wave number k approaches zero. All the other modes admit a cutoff frequency that occurs at

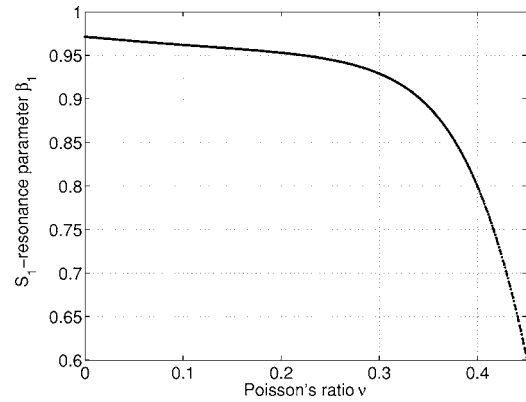


FIG. 2. First order symmetric Lamb mode S_1 . Variation of the resonance parameter β_1 vs Poisson's ratio ν .

$$f_c = n \frac{V}{2d}, \quad (2)$$

where n is an integer and V is equal to V_L or V_T according to the bulk acoustic wave involved in the mechanical vibration. At these frequencies, multiple reflections between the top and bottom faces of the plate result in a thickness resonance. The group velocity $V_g=d\omega/dk$ vanishes whereas phase velocity $V_\phi=\omega/k$ and Lamb mode wavelength $\lambda=2\pi/k$ become infinite. Such thickness vibration modes, uniformly distributed on the plate surface, are badly coupled to a local excitation resulting, for example, from a mechanical or a laser impact. Conversely, at the minimum frequency f_1 or f_2 of the dispersion curve of the first order symmetric (S_1) or second order antisymmetric (A_2) Lamb mode, the phase velocity V_ϕ and the wavelength $\lambda=V_\phi/f$ remain finite (Fig. 1). The conditions for the generation of local vibrations in a plate are much more favorable.

Depending on the value of Poisson's ratio ν , the cutoff frequency f_c of the S_1 Lamb mode is the smallest value of $V_L/2d$ and V_T/d . Since $V_T=V_L/2$ for an isotropic solid having Poisson's ratio $\nu=1/3$, we have

$$f_c = V_L/2d \quad \text{for } \nu < 1/3,$$

and

$$f_c = V_T/d \leq V_L/2d \quad \text{for } \nu \geq 1/3. \quad (3)$$

In both cases, the S_1 -ZGV resonance occurs at a frequency f_1 smaller than $V_L/2d$:

$$f_1 = \beta_1 \frac{V_L}{2d} \quad \text{with } \beta_1 < 1. \quad (4)$$

This parameter β_1 was incorporated in the American Society for Testing and Materials (ASTM) standards as a shape factor.¹² The value of this resonance parameter, which depends only on Poisson's ratio ν , can be deduced from the dispersion curves. Figure 2 shows that β_1 varies from 0.975 to 0.60 as Poisson's ratio ν varies from 0 to 0.451. For higher values of ν , no minimum frequency exists¹⁵ and the S_1 Lamb mode resonance occurs at the cutoff frequency $f_c=V_T/d$:

$$\beta_1 = 2 \frac{V_T}{V_L} = \sqrt{2 \frac{1-2\nu}{1-\nu}} \quad \text{for } \nu > 0.451. \quad (5)$$

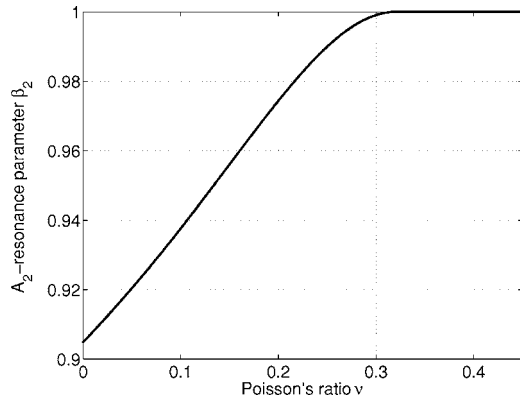


FIG. 3. Second order antisymmetric Lamb mode A_2 . Variation of the resonance parameter β_2 vs Poisson's ratio ν .

The cutoff frequency f_c of the A_2 Lamb mode is always equal to $3V_T/2d$. As pointed out by Negishi *et al.*, A_2 -ZGV point exists only for $\nu < 0.31$. The local resonance occurs at a frequency f_2 slightly smaller than $3V_T/2d$:

$$f_2 = \beta_2 \frac{3V_T}{2d} \quad \text{with } \beta_2 \leq 1. \quad (6)$$

Figure 3 shows that the A_2 -resonance parameter β_2 varies from 0.906 to 1 as Poisson's ratio ν varies from 0 to 0.31. For higher values of ν , no minimum frequency exists; the A_2 Lamb mode resonance occurs at the cutoff frequency and $\beta_2 = 1$.

The ratio f_2/f_1 of the two resonance frequencies is independent of the plate thickness d . It depends only on Poisson's ratio ν :

$$\frac{f_2}{f_1} = 3 \frac{V_T \beta_2}{V_L \beta_1} = 3 \sqrt{\frac{1-2\nu}{2(1-\nu)}} \frac{\beta_2(\nu)}{\beta_1(\nu)}. \quad (7)$$

Figure 4 shows that this ratio decreases from 1.975 to 1.5 as Poisson's ratio ν varies from 0 to 0.451. Since there is a one to one correspondence between f_2/f_1 and ν , the measurement of these two resonance frequencies provides an absolute determination of Poisson's ratio of the material. Then, using a polynomial interpolation of the curves plotted in Figs. 2 and 3, it is possible to calculate the resonance parameters β_1 and β_2 . Provided that the plate thickness d is known,

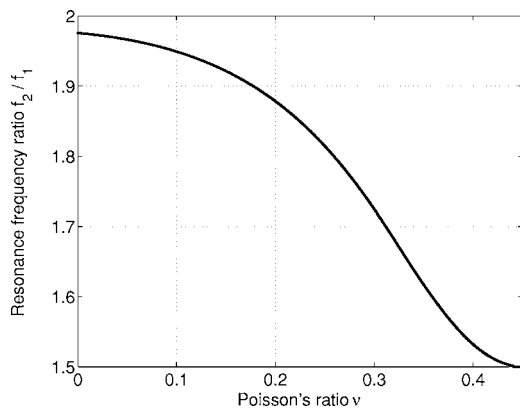


FIG. 4. Variations of the resonance frequency ratio f_2/f_1 vs Poisson's ratio ν .

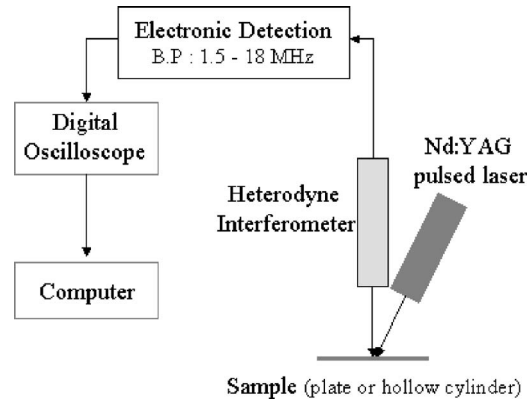


FIG. 5. Experimental setup.

Eqs. (4) and (6) allow us to determine the bulk acoustic wave velocities V_L and V_T and then the elastic constants c_{11} and c_{12} . This procedure, based on frequency measurements, is very accurate. Since the uncertainty on the resonance frequencies can be as small as 0.02%, the error depends mainly on the accuracy of the plate thickness measurement.

III. EXPERIMENTAL RESULTS

Using the experimental setup in Fig. 5, we have applied this method to many materials covering a large range of Poisson's ratios. Lamb waves were generated by a Q -switched Nd:YAG (yttrium aluminum garnet) laser providing pulses having a 20 ns duration and 4 mJ of energy. The spot diameter of the unfocused beam is equal to 1 mm. Prada *et al.* show that for a laser spot diameter equal to half the S_1 -ZGV wavelength λ_1 , the efficiency of the thermoelastic generation is much larger than for other Lamb modes.¹⁶ Numerical simulations show that the variations of the wavelength to thickness ratio (λ/d) versus Poisson's ratio ν are relatively small. For the S_1 Lamb mode: λ_1/d varies from 3.4 to 5 as ν varies from 0 to 0.4. For the A_2 Lamb mode: λ_2/d varies from 2.4 to 4 as ν varies from 0 to 0.27. In consequence, except for ν values closed to the limits where the ZGV resonances disappear, the optimal conditions are approximately fulfilled when the spot diameter is of the order of twice the plate thickness.

Lamb waves were detected by a heterodyne interferometer equipped with a 100 mW frequency doubled Nd:YAG laser.¹⁷ This interferometer is sensitive to any phase shift along the path of the optical probe beam. The calibration factor (10 nm/V) for mechanical displacement normal to the surface and the sensitivity (0.1 nm) were constant over a large detection bandwidth (50 kHz–40 MHz). Signals detected by the optical probe were fed into a digital sampling oscilloscope and transferred to a computer. As indicated in a previous paper,¹⁴ the laser energy absorption heats the air in the vicinity of the surface and produces a variation of the optical index along the path of the probe beam. The resulting phase shift induces a very large low frequency voltage, which saturates the electronic detection circuit. This spurious thermal effect and the low frequency oscillations corresponding to the A_0 Lamb mode are eliminated by interposing a high-pass filter having a cutoff frequency equal to 1.5 MHz.

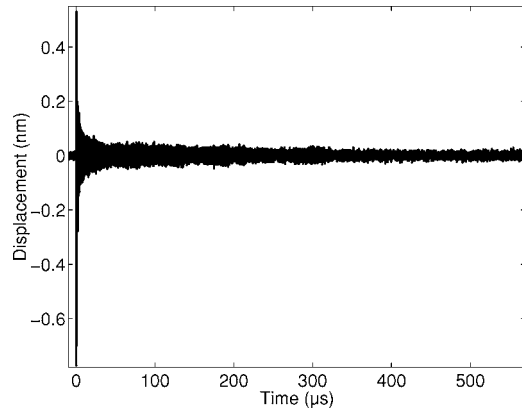


FIG. 6. Signal recorded at the same point on a steel plate of thickness $d = 900 \mu\text{m}$.

First experiments were carried out on a set of steel plates having lateral dimensions equal to 50 and 300 mm and calibrated thicknesses varying from 0.2 to 0.9 mm. The accuracy on the thickness is $\pm 2 \mu\text{m}$. Figure 6 is a typical example of the filtered time response recorded on a 0.9 mm thick plate. The spectrum shown in Fig. 7 was computed by a fast Fourier transform (FFT) of the first 200 μs of the signal. The two resonances are clearly observed. Assuming that the large peak at 3.081 MHz corresponds to the S_1 -mode ZGV resonance and the smaller one at 5.363 MHz to the A_2 -mode ZGV resonance, we can deduce from Eq. (5) Poisson's ratio ν and then the longitudinal and shear wave velocities.

The uncertainty Δf of the frequency measurement depends on the Q factor of the resonance, which is limited by the acoustic wave damping and by the time-window duration Θ used for computing the FFT. For usual solids, in the megahertz range, we observed that the Q factor is of the order of 1000, then with $\Theta = 600 \mu\text{s}$, we have $\Delta f \approx 1 \text{ kHz}$. For a given resonance frequency, the accuracy on Poisson's ratio ν and on the β parameter determination depends on the step p used to compute the curves in Figs. 2–4 and on the accuracy of the polynomial interpolation between the calculated

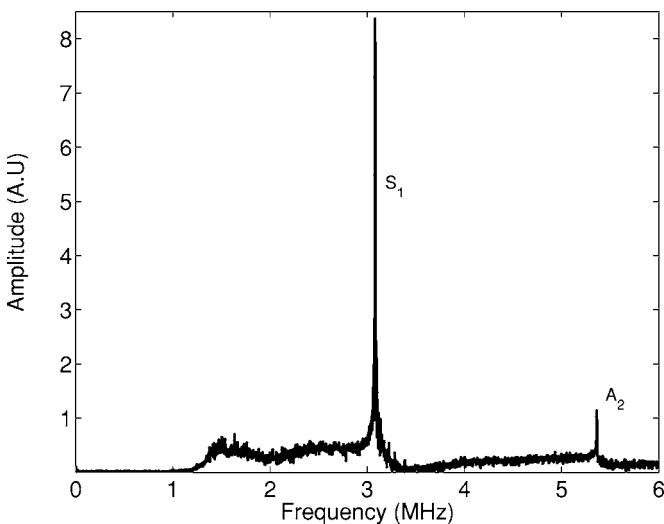


FIG. 7. Spectrum of the signal in Fig. 6. The peaks at 3.081 and 5.363 MHz correspond to the ZGV resonance of the S_1 and A_2 Lamb modes, respectively.

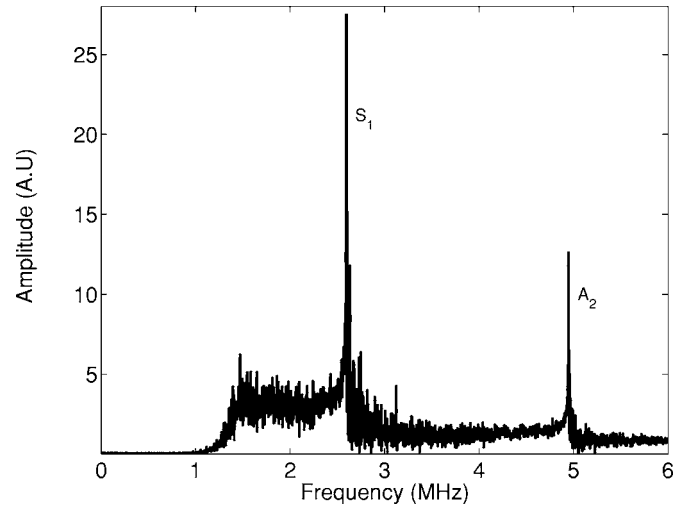


FIG. 8. Spectrum of the signal recorded on a fused silica plate of thickness $d = 1.100 \text{ mm}$ coated with a thin aluminum layer.

points. With $p = 0.001$ and a cubic interpolation, the relative uncertainty is of the order of 0.01%. Then, the relative uncertainty is equal to 0.1% for the β parameters and 0.2% for Poisson's ratio. For the steel plate under test, we found

$$\nu = 0.2918 \pm 0.0006,$$

$$\beta_1 = 0.9327 \pm 0.001 \text{ and } \beta_2 = 0.9982 \pm 0.001.$$

The longitudinal and shear wave velocities are deduced from the measured thickness ($d = 900 \pm 2 \mu\text{m}$):

$$V_L = 5946 \pm 20 \text{ m/s and } V_T = 3224 \pm 10 \text{ m/s}.$$

To partly confirm these results, the longitudinal wave velocity has been determined by classical pulse-echo technique with a 25 MHz contact piezoelectric transducer. The obtained value $V_L = 5960 \pm 30 \text{ m/s}$ is in good agreement with the previous ones.

BAW velocities have been measured for a large number of materials (copper, Duralumin, fused silica, steel, tantalum, tungsten, zinc). The plate thickness lies in the range of 0.3–1.1 mm. In all the experiments, the S_1 and A_2 -ZGV resonances appear, which allows us to determine the material parameters in a single shot. For most materials, the height of the A_2 mode ZGV peak is one order of magnitude smaller than the height of the S_1 -mode peak. As shown in Fig. 8, in the case of the fused silica plate, the amplitudes of the two peaks are comparable. This is due to the small value (0.172) of Poisson's ratio ν compared to that of steel (0.2918). Since the minimum of the A_2 Lamb mode dispersion curve is more pronounced for such small ν values (Fig. 9), the localization of the acoustical energy is improved.

Results are gathered in Table I. For each sample, we have checked that the longitudinal velocity is in good agreement (within 0.5%) with the value determined by classical pulse-echo technique. For some metals (copper, tungsten, zinc), relatively large discrepancies ($> 3\%$) with values given in the literature¹⁸ can be ascribed to the variations of their mechanical properties with the elaboration process. For example, in the case of fused silica, a well defined material,

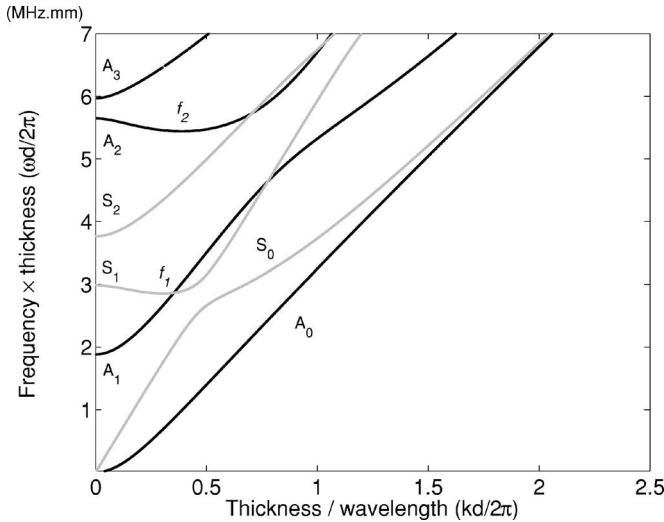


FIG. 9. Lamb wave dispersion curves for a fused silica plate ($\nu=0.172$). Compared to Fig. 1, the minimum of the A_2 Lamb mode dispersion curve is much more pronounced.

our values ($V_L=6005$ m/s and $V_T=3779$ m/s) are closed (within 0.5%) to the generally accepted ones: 5970 and 3765 m/s, respectively.

We observe that for a given acquisition time, the resonance peak width depends on material. Since the group velocity vanishes at the resonance, in a first order approximation, the energy is trapped within half a wavelength of the corresponding mode. Consequently, the width of the resonance is linked to the acoustic wave damping. This was shown in a preliminary study where the resonance width was used to determine the acoustic damping in Duralumin.¹⁴

The ZGV resonances have also been observed with the source and detection points on opposite faces. This configuration has the advantage of avoiding the spurious thermal signal and ensures a better signal to noise ratio, allowing measurements for thicker plate, resonating below 1 MHz. However, in practice, only one side of the structure under test might be accessible. In particular, this is the case for hollow cylinders. Elastic waves guided by the wall of a hollow cylinder are similar to Lamb waves, even for high values of the ratio b/a of external to internal radius. From the dispersion curves $\omega(k)$ calculated for hollow cylinders of Poisson's ratio 0.3,¹⁹ it can be shown that S_1 and the A_2 modes exhibit a horizontal slope for b/a up to 2. These curves also show that the parameters β_1 and β_2 vary with thickness.

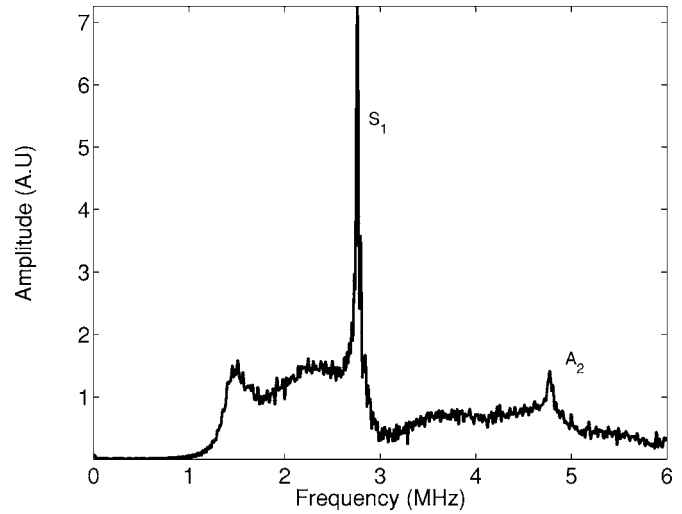


FIG. 10. Spectrum of the signal recorded on a steel hollow cylinder of diameter of 20 mm and shell thickness of 1.0 mm.

However, we consider that for thin shells, the values obtained for plates are good approximations. We have applied the ZGV resonance method on a steel cylinder with a diameter of 20 mm and thickness of 1.0 mm ($b/a=1.1$). The S_1 -ZGV and A_2 -ZGV resonances are very well detected, as observed in Fig. 10. Since the propagation of Lamb waves is not affected by the slight curvature of the surface, the velocities deduced from the resonance frequencies ($V_L=5942$ m/s and $V_T=3186$ m/s) are closed to the values measured on the steel plate, given in Table I. Conversely to the method proposed by Royer *et al.*⁸ no propagation around the shell is required. Consequently, the ZGV resonance method also applies to more complex structures than hollow cylinders.

IV. CONCLUSION

We have shown that the ZGV resonance that occurs at the minimum frequency of the S_1 and A_2 Lamb modes can be used for measuring Poisson's ratio and the longitudinal and shear wave velocities in thin plates or shells. Since the vibrations are excited in the thermoelastic regime by a laser pulse and detected at the same point by an optical interferometer, the measurement is local and is performed in a single shot on the same face of the structure, without any mechanical contact. This ZGV resonance method has been tested on

TABLE I. Poisson's ratio ν , resonance parameters β_1 , β_2 , and BAW velocities V_L , V_T determined by the ZGV resonance method for selected isotropic solids.

Material	ν	β_1	β_2	V_L (m/s)	V_T (m/s)
Copper	0.3245	0.9148	1.0000	4558	2323
Duralumin	0.3383	0.9036	1.0000	6370	3150
Fused silica	0.1720	0.9560	0.9643	6005	3779
Steel	0.2918	0.9327	0.9982	5946	3224
Stainless steel	0.2812	0.9367	0.9967	5635	3110
Tantalum	0.3314	0.9093	1.0000	4162	2090
Tungsten	0.2839	0.9357	0.9971	5395	2963
Zinc	0.2509	0.9450	0.9903	3607	2080

a large number of isotropic materials covering the usual range of Poisson's ratio. Since it is based on frequency measurements, the method is very accurate and the determination of Poisson's ratio is independent of the plate or shell thickness. For most of materials and taking into account the bandwidth of the laser pulse spectrum and of the optical probe (1–20 MHz), this method can be applied on plates or shells having thickness in the range of 0.2–3 mm. The ZGV resonance could be observed in much thinner membranes by using a picosecond laser and a high frequency optical probe. Compared to the temporal analysis used in picosecond acoustics, an important advantage of the ZGV resonance method is that it provides both the transverse and longitudinal velocities with a good accuracy.

¹M. J. Sansalone and N. J. Carino, NBSIR 86-3452, National Bureau of Standards, Gaithersburg, Maryland, Sept., 1986 (NTIS, PB#87-104444/AS).

²J. Krautkrämer and K. Krautkrämer, *Ultrasonic Testing of Materials* (Springer, Berlin, 1990).

³L. C. Lynnworth, *Ultrasonic Measurements for Process Control* (Academic, Boston, 1989).

⁴Z. Yu and S. Bosek, *Rev. Mod. Phys.* **67**, 863 (1995).

⁵D. Royer and E. Dieulesaint, *Elastic Waves in Solids* (Springer, Berlin, 1999), Vol. 1.

⁶J. D. Achenbach, *Wave Propagation in Elastic Solids* (North-Holland, Amsterdam, 1980).

⁷R. J. Dewhurst, C. Edwards, A. D. W. McKie, and S. B. Palmer, *Appl. Phys. Lett.* **51**, 1066 (1987).

⁸D. Royer, E. Dieulesaint, and Ph. Leclaire, *Proceedings of the 1989 IEEE Ultrasonics Symposium* (IEEE, New York, 1989), p. 1163.

⁹W. Gao, C. Glorieux, and J. Thoen, *Int. J. Eng. Sci.* **41**, 219 (2003).

¹⁰K. Van de Rostyne, C. Glorieux, W. Gao, W. Lauriks, and J. Thoen, *IEEE Trans. Ultrason. Ferroelectr. Freq. Control* **49**, 1245 (2002).

¹¹D. Holland and D. E. Chimenti, *Appl. Phys. Lett.* **83**, 2704 (2003).

¹²A. Gibson and J. S. Popovics, *J. Eng. Mech.* **131**, 438 (2005).

¹³C. Prada, O. Balogun, and T. W. Murray, *Appl. Phys. Lett.* **87**, 194109 (2005).

¹⁴D. Clorennec, C. Prada, D. Royer, and T. W. Murray, *Appl. Phys. Lett.* **89**, 024101 (2006).

¹⁵K. Negishi, *Jpn. J. Appl. Phys., Part 1* **26**, 171 (1987).

¹⁶C. Prada, O. Balogun, and T. W. Murray, *Proceedings of the 2005 IEEE Ultrasonics Symposium* (IEEE, New York, 2005) p. 1163.

¹⁷D. Royer and E. Dieulesaint, *Proceedings of the 1986 IEEE Ultrasonics Symposium* (IEEE, New York, 1986), p. 527.

¹⁸A. Briggs, *Acoustic Microscopy* (Clarendon, Oxford, 1992), p. 102.

¹⁹N. C. Nicholson and W. N. McDicken, *Ultrasonics* **29**, 411 (1991).